11th Australasian Fluid Mechanics Conference
University of Tasmania, Hobart, Australia
14-18 December 1992

FLOW MEASUREMENTS AND CALIBRATION OF A SUPERORBITAL EXPANSION TUBE

A.J. NEELY and R.G. MORGAN

Department of Mechanical Engineering
University of Queensland
QLD 4072, AUSTRALIA

ABSTRACT

A small pilot facility has been set up at The University of Queensland to demonstrate the concept of the Superorbital Expansion Tube, a free piston driven, triple diaphragm, impulse shock facility that utilizes the enthalpy multiplication mechanism of the unsteady expansion process. The pilot facility has been operated to produce quasi-steady test flows in air with shock velocities in excess of 13 kms^{-1} and with a duration of usable test flow approaching 15 μs. Experimental conditions with total enthalpies of 78 MJ and 106 MJ and total pressures of 15 and 37 Mpa respectively are reported. A flow model that accounts for non-ideal rupture of the light tertiary diaphragm is discussed. It is shown that equilibrium calculations more accurately model the unsteady expansion process than calculations assuming frozen chemistry.

INTRODUCTION

The Superorbital Expansion Tube is a free piston driven, triple diaphragm, impulse wind tunnel. This new hypervelocity facility is designed to produce flow conditions in a variety of test gases at velocities exceeding Earth orbital velocity. Even the most capable existing ground testing facilities such as free-piston driven shock tunnels and expansion tubes are limited in the maximum flow enthalpies they can produce. With the increasing interest in the design of vehicles to be used to enter the atmosphere of other planets or return to Earth's atmosphere from beyond Earth orbit, experimental facilities such as the Superorbital Expansion Tube will be required to allow aerodynamic ground testing of flight vehicle concepts and components. This paper outlines experiments in a small pilot facility in operation at The University of Queensland which has been used to demonstrate the capabilities of a Superorbital Expansion Tube using air as the test gas. The techniques used to model the flow processes involved, particularly around the tertiary diaphragm are also discussed.

PRINCIPLE OF OPERATION OF THE FACILITY

The operation of the Superorbital Expansion Tube is described in Morgan & Stalker (1991). It uses the phenomenon of enthalpy multiplication of the test flow through an unsteady expansion as used in the standard expansion tube, described originally by Resler and Bloxsom (1952). The total enthalpy of the flow is determined by the extent of this final unsteady expansion of the test gas.

The facility with secondary driver, shock tube and acceleration tube sections all of constant area (38 mm), is shown in Figure 1. The tunnel is driven by a helium filled, free piston driver which is used to shock heat a helium filled secondary driver section (2.111 m), separated from it by a heavy diaphragm (52.5 Mpa burst pressure).

The facility can be operated in two driver modes. In the first or *reflected* mode the driver gas is stagnated at the end of the secondary driver section and exhausts into the test gas contained in the shock tube section (of adjustable length, initially 3.150 m), which is separated from the secondary driver by a thin steel secondary diaphragm (1mm, 12.4 Mpa burst pressure). In the second or *straight-through* mode the thin steel secondary diaphragm is replaced with a light cellophane diaphragm (23 μm, 90 kPa burst pressure) which ruptures with the arrival of the shock. The second mode is the preferred mode of operation. Because the primary shock speed is overtailored, the reflection of the shock in the first mode would be expected to contaminate the driver gas.

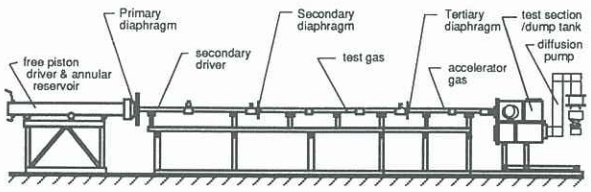

Figure 1. pilot Superorbital Expansion Tube facility

In both modes the resulting shock wave propagates into the shock tube and accelerates the quiescent test gas. The shock wave traverses the shock tube and ruptures the light tertiary diaphragm (9 μm grocery wrap, 20 kPa burst pressure) and then accelerates to a higher velocity as it passes into low pressure accelerator gas (helium or air) contained in the acceleration tube (1.289 m). The test gas following the shock is also further accelerated as it is expanded unsteadily into the acceleration tube. At the exit of the acceleration tube the test gas passes over the model mounted in the test section. Helium is the preferred accelerator gas as it has a low density and subsequently lower Mach number giving lower pressure and temperature ratios than air for the same shock speed.

It is the addition of the secondary driver section which, under the appropriate operating conditions, is able to boost the performance of the facility beyond that of a standard free piston driven expansion tube as reported by Neely and Stalker (1991). In an expansion tube the performance of the facility, that is the flow enthalpy that can be produced, is a function of the strength of the initial incident shock wave produced by the driver. Morgan and Stalker (1992) describe the performance enhancing mechanism of the secondary driver with the use of a wave diagram of the flow (Fig. 2).

The primary and secondary driver gases in regions 2 and 3 respectively, which are both helium have the same pressure and velocity. Thus if the free piston driver is operated so that the primary shock is overtailored then the helium in region 2 will have the higher speed of sound and will thus be able to drive a higher shock speed through the test gas contained in the adjacent shock tube than would be possible for a single driver arrangement where region 3 drives the test gas shock directly.

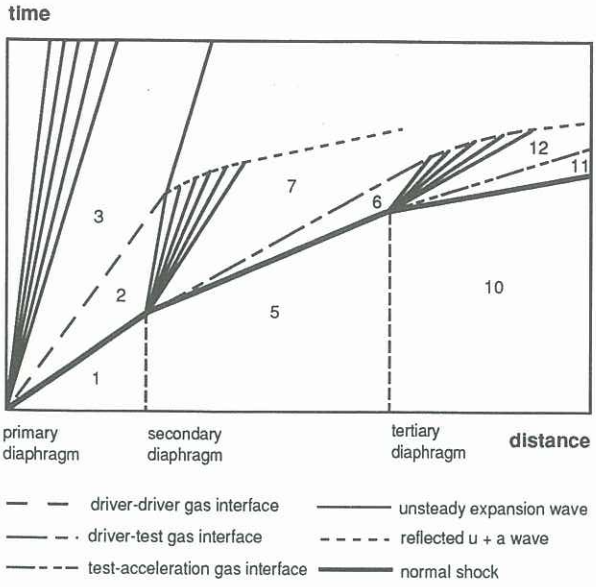

Figure 2. wave diagram of SEXT flow process

EXPERIMENTAL TESTING

To investigate the performance of the Superorbital Expansion Tube concept, a series of runs were carried out in the pilot facility using a range of filling pressures in the secondary driver (40-200 kPa), shock tube (150-10000 Pa) and acceleration tube (1-380 Pa) sections. Two distinct experimental conditions produced in the facility are set out in Table I.

Table I. experimental conditions

flow condition		78 MJ	106 MJ
run number		220	231
secondary driver fill pressure	(kPa)	60	60
shock tube fill pressure	(Pa)	500	800
acceleration tube fill pressure	(Pa)	17	10
accelerator gas		air	He
shock tube length	(m)	3.150	1.625
final primary shock speed	(ms^{-1})	6 450	-
final secondary shock speed	(ms^{-1})	6 880	7 280
final tertiary shock speed	(ms^{-1})	10 500	13 000

For the lower enthalpy condition, with a final tertiary shock velocity of 10.5 kms^{-1}, a period of quasi-steady flow in excess of 50 µs was observed. It was observed that for the high shock velocities produced in the shock tube (> 8 kms^{-1}) there was severe attenuation of the flow with the shock being slowed by up to 2 kms^{-1} when it reached the tertiary diaphragm. To avoid the resulting decrease in performance due to flow attenuation, sections of the shock tube were removed to reduce its length (to 1.625 m) so that the secondary shock reaches the tertiary diaphragm before any significant attenuation has occured. The second condition was produced with this configuration. Final tertiary shock velocities in excess of 13 kms^{-1} were achieved where a period of quasi-steady usable test flow of 15 µs duration was observed.

Static pressure levels were recorded at a number of stations down the length of the three sections. A typical record of wall static pressures measured in the acceleration tube is shown in Figure 3, illustrating the development of a region of steady flow between the tertiary shock wave and the trailing expansion wave, which terminates the test flow, as the flow is expanded.

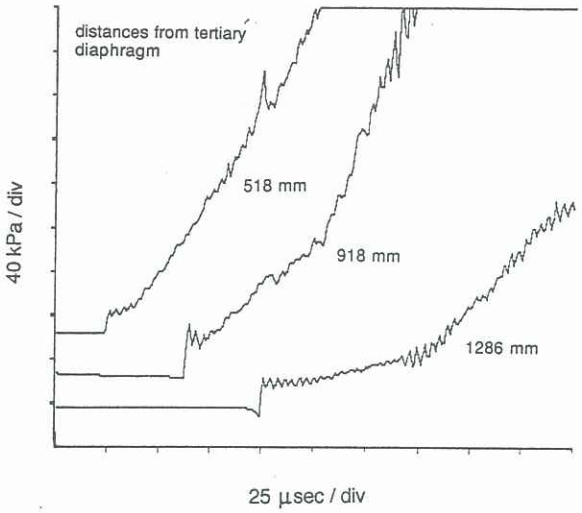

Figure 3. acceleration tube wall static pressure histories for 78 MJ condition

A standard PCB piezoelectric pressure transducer, shielded from the direct flow, and an aluminium/lead bar gauge, utilising piezoelectric film, were used alternately to measure the centreline pitot pressure levels in the test flow. Typical wall static pressure and centreline pitot pressure histories recorded at the exit of the acceleration tube are shown in Figure 4 for the two different enthalpy conditions. For the 106 MJ condition the static pressure trace shown is from an equivalent run (R226) as the exit trace was corrupted. High frequency oscillations visible on the traces are consistent with ringing of the gauges and are not a flow phenomenon.

Pitot pressure levels were observed to rise during the period of test flow as expected from the analytical model of the test flow which predicts non uniform gas states in region 8. The calculated pressure levels that bound these test flows are indicated on Figure 4 and can be seen to follow the observed behaviour. As can be seen from the pressure traces, problems were experienced with the rise time of the gauges used to measure the pitot pressure. In the case of the PCB gauge this was due to the filling of the cavity between the transducer and its shield. While the bar gauges, which were custom made, do not require protective shielding, calibration tests indicate long rise times of 4 - 6 µs. Development of the bar gauges is continuing in house, and an improved response is anticipated.

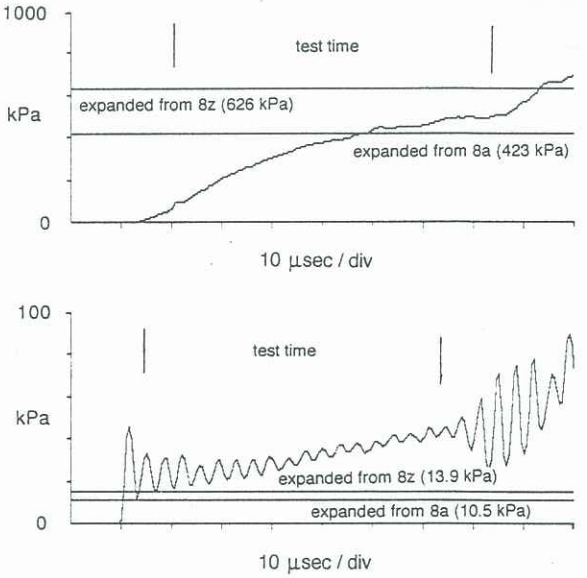

Figure 4 (a) centreline pitot pressure histories and corresponding exit wall static pressure histories for 78 MJ test condition

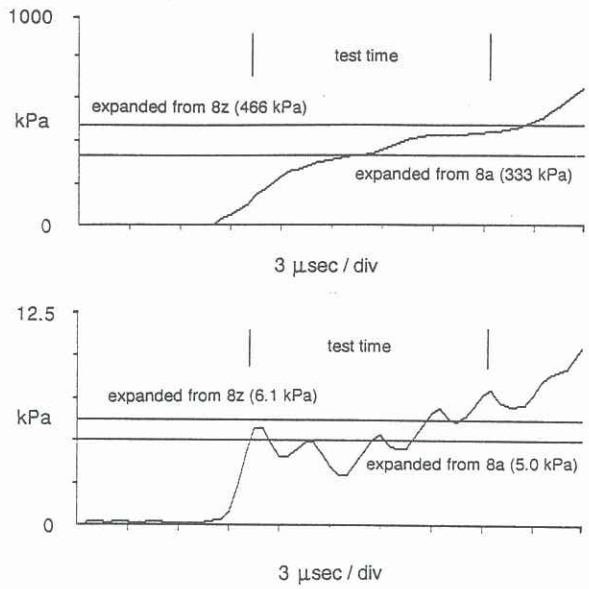

Figure 4 (b) centreline pitot pressure histories and corresponding exit wall static pressure histories for 106 MJ test condition

ANALYSIS OF THE FLOW

This paper deals with the analysis of the flow of test gas through the shock tube and acceleration tube resulting in the final test flow in the test section. No attempt is made here to model the driver flow although the perfect gas analysis from Morgan and Stalker (1992) was used to help determine the optimum driver conditions.

The observed shock speeds in the shock and acceleration tubes are used in conjunction with the known quiescent test gas pressures in these two sections to calculate the secondary and tertiary shock strengths. Real gas calculations of these conditions are made using an equilibrium analysis. The static pressure and the entropy level behind the shock are determined and these are used to determine the full gas state via an equilibrium scheme (Rizkalla 1990).

It should be noted that although the shock heated test gas in region 6 is nominally indicated as being a region of uniform flow in Figure 5, it is in fact a region in which there is a velocity gradient induced by viscous effects. The Mirels analysis (1962) was used to predict the velocity of various points in the the region and this was found to have a significant effect on the final values of pitot pressure calculated for the expanded test flow.

The lightest possible tertiary diaphragm is used to separate the air test gas and the helium accelerator gas. Ideally this diaphragm would rupture instantaneously and would have no further influence on the flow. But as has been reported in previous expansion tube work (Shinn and Miller 1977) even the lightest diaphragm does not behave ideally resulting in two principal non-ideal effects. These are reflection of the incident secondary shock wave into the oncoming test gas before the diaphragm ruptures and momentum loss from the expanded flow due to the energy required to accelerate the diaphragm mass after rupture. This nonideal behaviour can be observed on a more detailed wave diagram for the flow in the vicinity of the tertiary diaphragm (Fig. 5).

These non-ideal effects must be accounted for and have a significant influence on the calculated test gas conditions. The slug of shock heated test gas that arrives at the tertiary diaphragm (Fig.5, region 6) is processed by the reflected shock wave (region 8) and then passes through the unsteady expansion which develops behind the accelerator-test gas interface. The source of shock heated test gas for the expansion is non uniform. The first part of the test gas slug to arrive (region 8a), is stagnated by the shock that is reflected from the tertiary diaphragm and is then expanded from this state. Once the diaphragm ruptures though, this stagnation of the flow no longer occurs as the reflected shock is washed downstream by the flow and the reflected shock attenuates (region 8b..z). The test gas is thus expanded from a range of initial states .

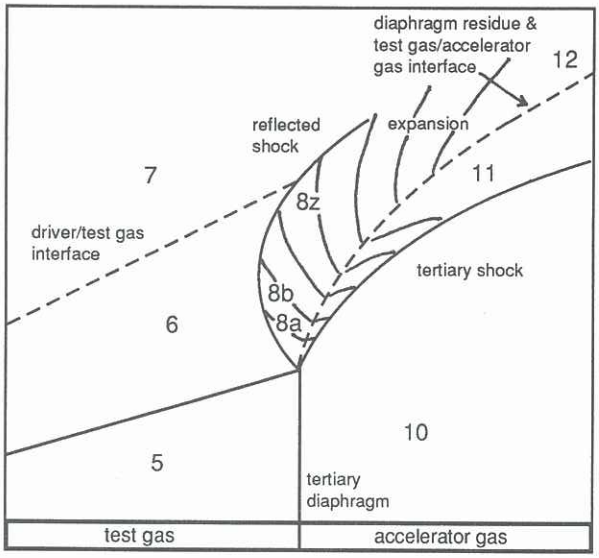

Figure 5. wave diagram for the flow near the tertiary diaphragm

Calculation of the expansion process and the resulting state of the test gas must thus be made for a range of starting conditions. It is perhaps easiest to consider the two bounding extremes of the starting flow. The first is the initial part of the test gas slug (region 8a) which is taken as initially stationary with conditions determined for a fully reflected shock bringing the gas to rest. The other extreme is the terminating case (region 8z) where the interface separating the test gas and secondary driver gas catches up with the attenuated reflected shock. The calculation of this state is less straightforward.

To determine the strength of the reflected shock at interface catchup it is necessary to model the behaviour of the tertiary diaphragm after rupture. The residual influence of the tertiary diaphragm after rupture is represented by the inertia of the diaphragm as it is washed downstream (Morgan and Stalker 1992) in a similar form to the action of a free piston. The mass of the ruptured diaphragm is accelerated downstream by the pressure behind the reflected shock. As this occurs expansion waves propagate upstream from the diaphragm, eventually attenuating the reflected shock to a Mach wave. The accelerating diaphragm also sends compression waves downstream into the accelerator gas which converge to form the tertiary shock.

As the reflected shock and the diaphragm are initially in close proximity and the sound speed behind the reflected shock is very high, it is assumed that the expansion waves emanating from the diaphragm immediately catch up with the reflected shock, thus specifying a region of uniform gas velocity between the reflected shock and the diaphragm remnants. The velocity of the diaphragm remnants is determined by the integration of its acceleration from rupture. The diaphragm velocity may then be used with the known incoming test gas velocity to determine the strength of the shock at each moment. As the reverse shock traverses the test gas it induces an entropy change in the gas which must be determined. The period it takes the shock to traverse the slug of test gas is small (< 15 µs) and it can be shown that only a small displacement of the diaphragm will occur in this time indicating that it is permissible to determine the reverse shock strength from simple theory. It should also be noted that as the initial pressure loadings on the tertiary diaphragm are small (less than 1/25th of the burst pressure) there will be no significant pre-deformation of the diaphragm suggesting one dimensional behaviour and circumferential failure of the light diaphragm material.

To determine the velocity of the gas behind the attenuated reverse shock at the point of interface catchup, it is assumed via Mirels (1963) theory that the velocity of the test flow contained between the reflected shock and the upstream interface is matched to the velocity of the interface. The gas velocity across the shock is calculated and is then expanded through the unsteady expansion.

Once these starting conditions are determined the remnants of the diaphragm on the flow are disregarded as they can have no further effect on the flow entropy. The two starting conditions are used to calculate the limits of the range of test gas flows produced at the end of the unsteady expansion. Calculation of the changing state of the flow through the unsteady expansion is implemented in a stepwise manner. The expansion process is divided up into a large number (100) of velocity increments which proceed from the calculated starting velocity of the test gas (State 8) to the final velocity after expansion (State 12). This final velocity is set equal to the observed tertiary shock speed by the assumption of full Mirels development of the slug length in the accelerator gas. Calculation across each increment is governed by the standard equation for an unsteady expansion wave which relates the change in static enthalpy to the change in velocity and the local speed of sound.

$$dh = - a\,du \qquad (1)$$

A calculation of the entropy and static enthalpy of the flow is made at the initial state 8. For equilibrium or frozen flow the expansion is isentropic. The gas condition is uniquely defined by the enthalpy and entropy and the EQSTATE code (Rizkalla 1990) is used to iterate, at the end of each computed step, a solution for pressure, temperature and gas composition. The CREK subroutines developed by Pratt and Wormeck (1976) are used to calculate the equilibrium composition at each point. The process proceeds until the final velocity is reached, thus supplying the final state of the test gas. The calculated gas states of the test flow (region 12) at the end of the acceleration tube, are set out in Table II for the two enthalpy conditions discussed in the previous section.

Table II. final test flow states calculated using equilibrium and frozen theory

flow condition	78 MJ		106 MJ	
calculation method	equilib.	frozen	equilib.	frozen
velocity (ms^{-1})	10 500	10 500	13 000	13 000
temperature (K)	5 901	236	5 526	8
pressure (Pa)	13 914	96	6 103	0.017
density ($10^{-2}\,kgm^{-3}$)	0.57	0.072	2.76	0.0004
Mach number	5.7	20.1	7.4	95
ratio of spec. heats	1.40	1.64	1.39	1.62
pitot pressure (kPa)	626	79.8	466	0.6
total pressure(MPa)	15.2	31.0	37.4	16.2

The resulting calculation of static and pitot pressure levels for each starting condition can also be seen in Figures 4a. and 4b., superimposed on those pressures measured in the experimental flow. A comparison can be made here with the effect of assuming a frozen expansion process. Calculations of the expanded state of the test gas required to match the observed final velocity for a frozen expansion were made by fixing the chemical state of the test gas after processing by the reflected shock (State 8). The resulting expanded states are set out in Table II. It can be seen that the resulting temperatures and static and pitot pressures of the expanded test gas are unrealistically low giving support to the assumption of an approximately equilibrium process occurring through the unsteady expansion. It can thus be seen that to achieve the high enthalpy flow conditions produced by the Superorbital Expansion Tube in experiments, the flow energy used to dissociate the test gas when it is shock heated in the shock tube must be at least partially restored to the flow through recombination of the test gas through the unsteady expansion. If this energy remained frozen as chemical energy the observed test conditions could not be achieved. In the Superorbital Expansion Tube, the total enthalpy is not fixed at any point in the flow as it is in shock tunnel facilities. Rather it relies on the enthalpy multiplication mechanism of the unsteady expansion and thus any increase in energy due to recombination through the unsteady expansion will be multiplied by the expansion to produce the elevated final enthalpies recorded.

CONCLUSIONS

A small pilot facility has been set up at The University of Queensland to demonstrate the concept of the Superorbital Expansion Tube, a free piston driven, triple diaphragm, impulse facility. The pilot facility has been operated to produce quasi-steady test flows with shock velocities in excess of 13 kms^{-1} and with a duration of usable test flow of 15 μs. Such high enthalpy flows are of interest in the design of any vehicle used to traverse an atmosphere at velocities exceeding Earth orbital velocity.

Consideration of the effects of boundary layer growth and non ideal diaphragm rupture on the flow have allowed a better understanding of the flow mechanism and enabled more accurate matching of calculated and observed test flow states. It has also been shown conclusively that much better agreement with experiment is achieved if the unsteady expansion process is modelled as an equilibrium process rather than as a frozen chemistry process.

These initial results have demonstrated the viability of the Superorbital Expansion Tube concept and while further testing on the pilot facility will continue, work is now proceeding on the design of a larger scale, medium size facility at The University of Queensland.

ACKNOWLEDGEMENTS

The authors gratefully acknowledge the financial support of the Australian Research Council.

REFERENCES

MIRELS, H (1963) Test Time in Low -Pressure Shock Tubes. The Physics of Fluids, 6.9

MORGAN R G and STALKER R J (1992) Double Diaphragm Driven Free Piston Expansion Tube. Proceedings of the 18th International Symposium on Shock Waves, Sendai 1991

NEELY A J, STALKER R J and PAULL A (1991) High enthalpy, hypervelocity flows of air and argon in an expansion tube. The Aeronautical Journal, June/July, 175-186

PRATT, D T and WORMECK, J J (1976) CREK: A computer program for calculation of combustion reaction equilibrium and kinetics in laminar or turbulent flows. Report WSU-ME-TEL-76-1, Washington State University

RESLER, E L and BLOXSOM, D E (1952) Very High Mach Number Flows By Unsteady Flow Principles, limited distribution monograph, Cornell University Graduate School of Aeronautical Engineering

RIZKALLA, O (1990) EQSTATE: program to calculate the equilibrium or frozen properties of a supersonic gas flow at the static and stagnation points upstream and downstream of a shock wave. General Applied Science Laboratories Inc., New York

SHINN, J L and MILLER, C G, (1978) Experimental Perfect-Gas Study of Expansion-Tube Flow Characteristics. NASA Technical Paper 1317